MICROSTRUCTURE OF 08CH18N10T AUSTENITIC STEEL AFTER THERMO-MECHANICAL FATIGUE TESTS

JANDOVÁ Dagmar[1*], FEKETE Balazs[2], KASL Josef[1], JÓNI Bertalan[2]

[1]Research and Testing Institute Pisen, Pilsen, Czech Republic, EU, jandova@vzuplzen.cz
[2]College of Dunaujvaros, Dunaujvaros, Hungary, EU,

Abstract

The fatigue properties and microstructure of 08Ch18N10T steel used for production of the interior of a pressure water reactor VVER 440 were investigated. The influence of the service conditions was simulated using thermo mechanical strain controlled low cycle fatigue tests in the range from 150°C to 270°C. The cyclic stress behaviour was investigated at different total strain amplitudes. The cyclic test to rupture and fractographic analysis were carried out. Selected tests were interrupted at different stages of fatigue life and changes in microstructure were evaluated. Dislocation density was determined using transmission electron microscopy and X-ray diffraction. Dislocation rich and dislocation poor regions appeared as a result of cyclic loading. Vein structure and successive formation of persistent slip bands and dislocation cells were observed similar to those in FCC metal monocrystals fatigued at room temperature. Dislocation density increased considerably at the beginning of cyclic loading; maximum was reached at 0.05 of life time. The following gradual decrease was related to rearrangement of dislocations into the walls. Simultaneously the nature of the dislocations changed. A majority of the screw dislocations occurred in as received conditions and at the beginning of cyclic loading. The fraction of edge dislocations increased with the increasing number of cycles. Distance between persistent slip bands and size of dislocation cells were related to the distance between striations on the fracture surface.

Keywords: Low cycle fatigue, austenite, dislocation substructure, X-ray diffraction, transmission electron microscopy

1. INTRODUCTION

Corrosion resistant 08Ch18N10T austenitic stainless steel (ASTM equivalent AISI 321) is chromium-nickel steel stabilized with titanium against carbide precipitation and designed to work within the temperature range, where carbide precipitation can develop. Stabilized at temperatures between 950°C and 1010°C the steel resists scaling and vibration fatigue. It is used for production of various components of the pressure water reactor VVER 440. Being exposed to cyclic temperature and pressure during transient operation the steel microstructure undergoes irreversible changes, which can result in strength decrease, crack nucleation and propagation. The life time of individual components is usually predicted on the basis of the standard isothermal fatigue (IF) tests, however thermal variations cause additional internal stresses that can accelerate microstructural processes and shorten the life time [1]. Therefore thermo-mechanical fatigue (TMF) tests were carried out which simulate possible service conditions in the pressure water reactor. They can represent material behaviour near the surface layers of the component caused by cyclic temperature and pressure, in subsurface layers of the components due to an inhomogeneous temperature field and in the walls of pipes or vessels due to the inhomogeneous temperature of the flowing media [2].

The paper deals with microstructural investigation of 08Ch18N10T steel after low cycle thermo-mechanical fatigue tests. Developments of dislocation substructure at different stages of fatigue life and fracture mechanisms were evaluated.

2. EXPERIMENTAL PROCEDURES

Specimens for fatigue tests were machined out of tubes made of 08Ch18N10T steel (**Table 1**). Cylindrical specimens of 8 mm gauge diameter and 7 mm length were tested using a GLEEBLE thermo-mechanical simulator. The test was run under uniaxial tension - compression loading with total strain control. All fatigue tests were carried out at a frequency of 0.083 Hz and a triangular waveform. The longitudinal total strain was controlled by a HZT060 type linear displacement transducer at different levels of total strain amplitude (TSA) from 0.9 to 2.0 %. A K-type thermocouple was welded in the middle of the gauge length to control and measure the temperature of the test specimen. The TMF tests in a temperature a range from 150°C to 270°C were carried out in the in-phase conditions and with a heating and a cooling rate of 20 °C/s. Temperature and stress cycling is evident in **Fig. 1**.

Table 1 Chemical composition of 08Ch18N10T steel

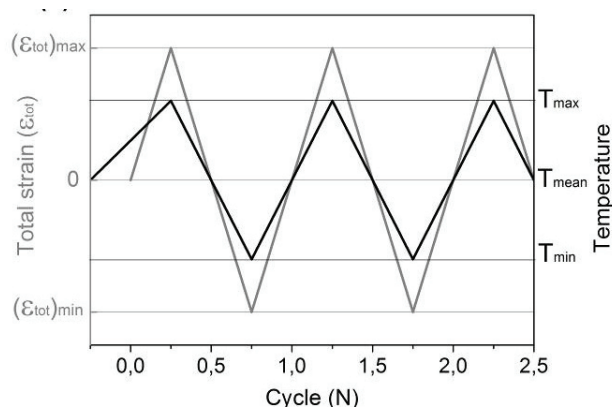|	C	Si	Mn	S	P	Cr	Ni	Ti
Nominal	max 0.08	max.	1.0 -	max. 0.020	max. 0.035	17.0-19.0	9.0-	min. 5xC-
Actual	0.06	0.63	1.64	<0.004	0.026	17.78	9.99	0.5

Fig. 1 Input profiles of thermo-mechanical cycles

Four fatigue tests with a different total strain were automatically stopped when the failure criterion was reached, which was chosen to decrease the maximal cyclic load in the tension phase by 25 %. Then the test bars' surfaces were observed to evaluate the number, size and distribution of cracks using light and scanning electron microscopy. Then the bars were loaded by tension in a tensile test machine to break them and fracture surfaces were observed using scanning electron microscopy (SEM).

The next four specimens with a strain amplitude of 1.2 % were tested up to 5 %, 25 %, 50 % and 70 % of cumulative usage factor (CUF) that represents life fraction. The dislocation substructure of these specimens was evaluated using transmission electron microscopy (TEM) and X-ray diffraction (XRD) in order to elucidate the kinetics of the TMF process and to correlate the mechanical response and the material's microstructure evolution.

3. RESULTS AND DISCUSSION

3.1. Fatigue tests

The cyclic stress response of the tested material is shown in **Fig. 2**. Other results including comparison of TMF tests with isothermal fatigue tests at 260°C will be published [3]. In the strain controlled low cycle fatigue, the cyclic stress behaviour is one of the most important features of the material, as it represents the path of the

stress amplitude during the fatigue life. The cyclic stress response of the material investigated is shown in **Fig. 2** for different total strain levels.
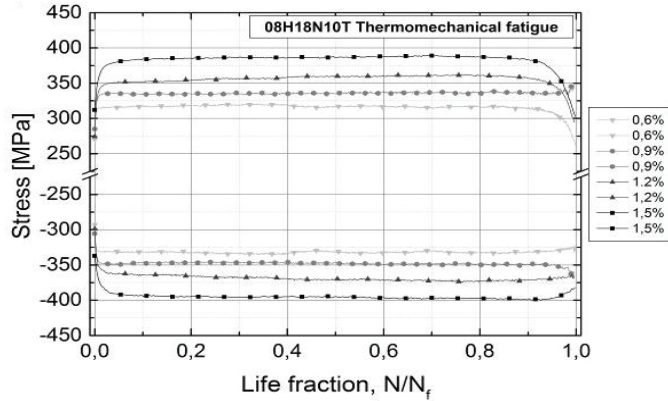

Fig. 2 Cyclic stress response of the tested material. N represents actual number of cycles and N_f number of cycles to rupture

Three different stages of the cyclic stress responses at all strain ranges and temperature levels can be distinguished. Cyclic hardening occurred at the beginning of the fatigue test, which is typical for austenitic stainless steels under strain-controlled LCF conditions [1, 2]. This first stage was observed up untill about 0.05 of life fraction and stress increase was more significant at higher strain amplitude levels. The second quasi-stabilized stress stage lasts up to about 0.9 of life time fracture. The following softening is related to cracks nucleation and propagation.

3.2. Dislocation substructure

The microstructure of the 08Ch18N10T steel consists of austenitic grains of about 100 μm containing many twins, coarse primary titanium carbonitrides, δ-ferrite particles of several tens of micrometers and $M_{23}C_6$ carbides. These carbides predominately occupied grain boundaries. Non-uniform distribution of fine titanium carbonitrides was observed within austenite grains.

The dislocation substructure was observed using thin foils prepared from central cross section plates of fatigued specimens thinned to electron transparency by means of jet electrolytic polishing in 6 % solution of $HClO_4$ in methanol at a voltage of 22 V and a temperature in a range from -65°C to -55°C. Dislocation density was determined using the Keh-Weismann´s intersection analysis [4]. A rectangular grid was put on the TEM micrograph and intersections with dislocations were counted. Then dislocation density ρ was determined using the formula

$$\rho = \left(\frac{n_1}{L_1} + \frac{n_2}{L_2} \right) \cdot \frac{x}{t} ,$$

(1)

where n_1 and n_2 are numbers of intersections of dislocation lines with two systems of parallel lines of a total length L_1 and L_2 respectively, x is the factor of visibility that depends on the nature of dislocations and t the thickness of the foil. Dislocation density was evaluated using micrographs taken at two-beam conditions with a strong 111 reflection. The corresponding extinction distance ξ_g = 28.27 nm for observation at an accelerated voltage of 120 kV was calculated on the basis of published value ξg = 33.5 nm for AISI 316 stainless steel observed in TEM at an accelerated voltage of 200 kV steel [5]. Factors of visibility 1 and 2 were used for edge and screw slip dislocations respectively [6]. In addition, cell substructure was evaluated using equivalent diameter as the cell size parameter.

Dislocation substructure of the steel in as received conditions consisted of a disordered dislocation network with a low dislocation density of 0.7 $\cdot 10^{14}$ m^{-2} (**Fig. 3a**). Dislocation-poor and dislocation-rich areas were formed

during the cyclic deformation similar to those, which were observed in fatigued monocrystals of FCC metals [7]. The dislocation substructure observed in individual austenitic grains in polycrystalline steel depended on their crystallographic orientation and relation to applied stress. Dislocations concentrated in areas called veins separated by channels are shown in **Fig. 3**, which were taken in a grain orientated near the [110] pole. According to the model published by Mughrabi the vein substructure consists of bundles of edge dislocations and channels containing some screw dislocations [8]. Such structure precedes formation of persistent slipbands (PSB) and dislocation cells [7].
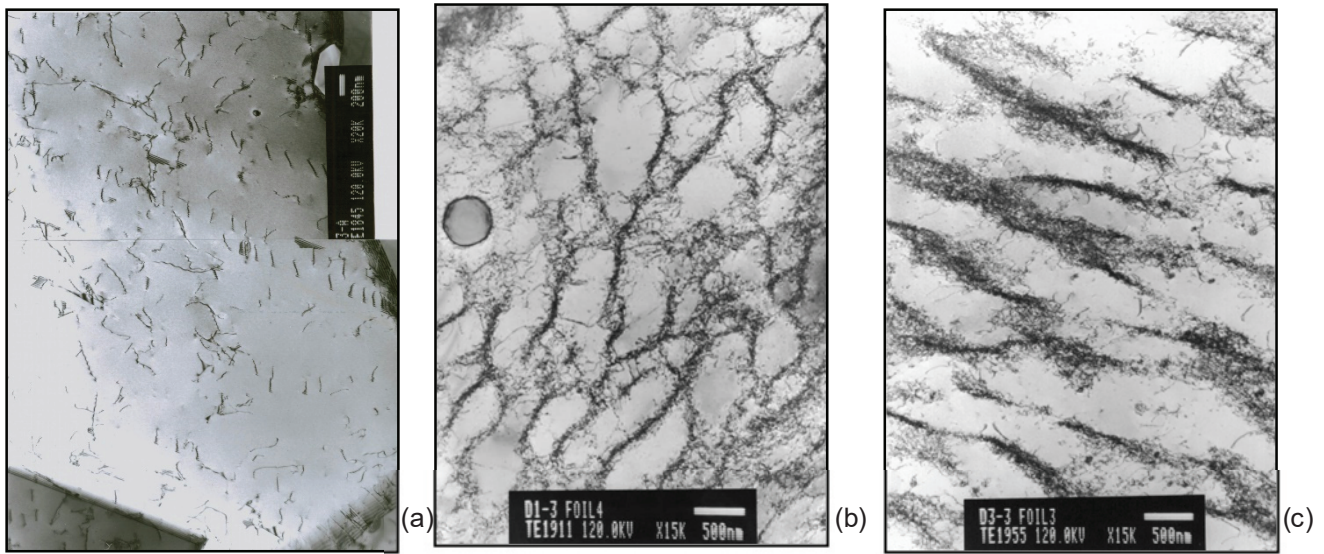

Fig. 3 Dislocation substructure of fatigued specimens: a) CUF = 0%, b) CUF = 5%, c) CUF = 25%. TEM
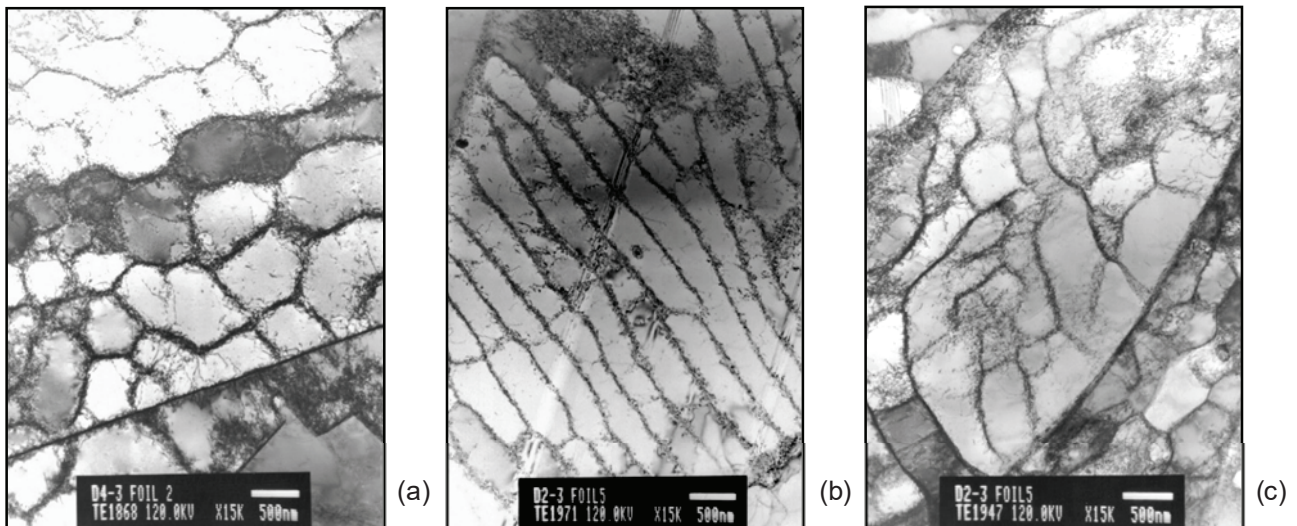

Fig. 4 Dislocation substructure of fatigued specimens: a) CUF = 50%, b) and c) CUF = 70%. TEM

Transition from veins into persistent slip bands is shown in **Fig. 3c** taken in orientation near the pole [123]. The width of veins decreased the number of cycles increased and the persistent slip bands (PSB) were formed. Cell substructure was observed in grains if two slip systems were activated as shown in **Fig. 4a** of the grain orientated near [012] pole. Wavy persistent slip bands separated by dislocation-poor channels occurred in grains, where only one slip system was active (**Fig. 4b**). Therefore well-developed cell substructure as well as

structure with persistent slip bands was observed in one specimen. Wavy persistent slip bands seemed to pass into a labyrinth-type substructure [7] in advanced stages of fatigue life (**Fig. 4c**).

Dislocation densities in fatigued samples were measured separately for dislocation-rich and dislocation-poor areas. The nature of dislocations was taken into account. It was assumed according to the literature [9] that edge dislocations occurred in dislocation-rich areas (veins, persistent slip bands or walls), while screw dislocations were present in dislocation-poor areas (channels or interior of cells). Total dislocation density was also determined using X-ray diffraction. Results are plotted against CUF in **Fig. 5a**. Conditions of X-ray diffraction measurement are described in another paper submitted for publication [3]. After an initial increase in dislocation density, a gradual decrease was seen; the course is similar for both measurement methods nevertheless dislocation density determined from TEM micrographs was relatively low. The reason may be firstly the difficulty of resolving individual dislocations in dislocation rich slip bands, secondly the dependence of dislocation visibility on its nature and thirdly too relatively small volume of material evaluated by TEM as TEM microscopy is a highly localized method. The nature of the dislocations was determined using analysis of the broadening of the X-ray diffraction lines. It was found that screw dislocations prevailed in as received conditions and in the specimen of 0.05 CUF, while edge dislocations prevailed in other fatigued specimens with CUF from 0.25 to 0.70 [3]. During fatigue life from CUF of 0.05 to 0.70 the size of dislocation cells decreased from 825 to 645 nm, while the distance of persistent slip bands did not seem to change; the value of 580 nm was determined for CUF of 0.70.
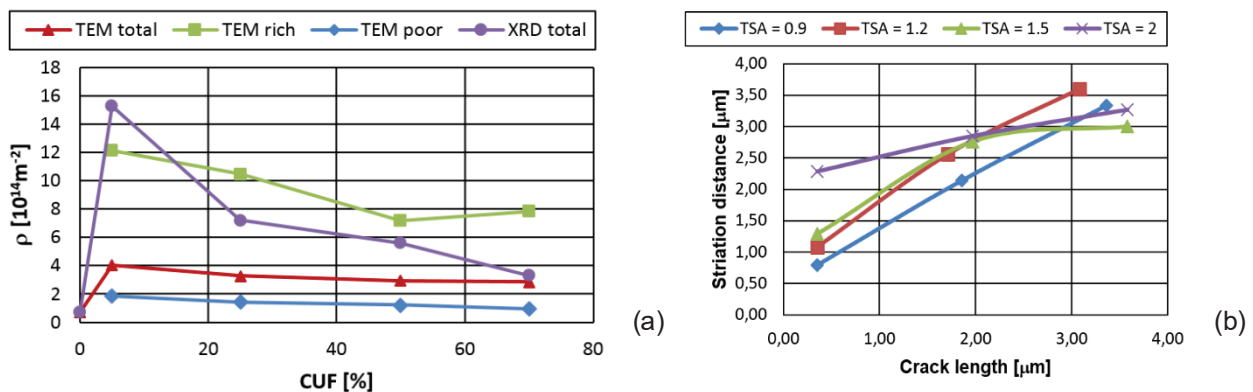

(a)

(b)

Fig. 5 Quantitative evaluation: a) dislocation density and b) striation distance
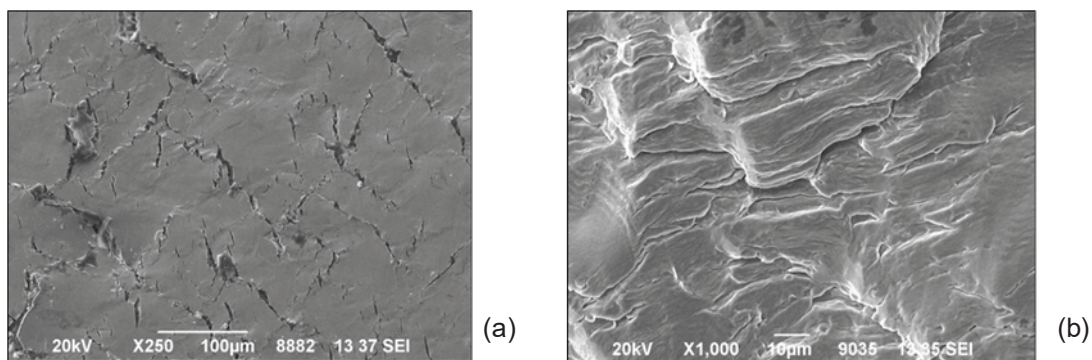

(a)

(b)

Fig. 6 Fatigued specimen with TSA = 2.0%: a) surface of the bar, b) fracture surface near the crack origin. SEM-micrographs

3.3. Fractography

Fatigued specimens showed several major cracks (for the low total strain amplitude) and a lot of cracks (for the higher total strain amplitude) originating on the surface of the test bars. These small cracks were often

connected to each other and formed a regular network. Bands with apparent plastic deformation were observed between individual cracks at high total strain amplitude (**Fig. 6a**). The striations were observed at fracture surfaces (**Fig. 6b**). The distance between them increased in the direction from the initiation center to the end of the crack (**Fig. 5b**).

4.   CONCLUSIONS

Strain controlled low cycle thermo-mechanical fatigue tests in a temperature range from 150°Cb to 270°C yielded shorter fatigue life compared to the isothermal fatigue tests at 260°C. The results will be used for the remaining life assessment of components of the pressure vessel reactor VVER 440.

The stress response at different strain levels revealed cyclic hardening and the degree of hardening was more significant at higher strain amplitude levels. The initial increase in hardening was caused by the generation of new dislocations. The following formation of persistent slip bands and dislocation cell substructure resulted in a quasi-stable stress response. The stress response remained the same up to 0.9 of fatigue life time in spite of a gradual decrease in dislocation density. The reason is that the dense dislocation walls within persistent slip bands and between dislocation cells act as strong obstacles for dislocation motion. The distance between persistent slip bands as well as the size of dislocation cells slightly decreased during fatigue tests and corresponded well with the size of striations at the fracture surface.

Fatigue cracks were initiated at the surface of fatigued specimens in places, where persistent slip bands meet the specimen surface. Interconnection of several major crack resulted in fracture. A lot of secondary cracks were created at the specimen surface and formed networks of small cracks and plastically deformed strips. Typical fatigue fracture surfaces with striations were observed. Near the initiation center the mean distance between striation lines increased with increasing crack length and then it became saturated. The size of striations near the initiation center of fracture was only slightly higher than the distance between persistent slip bands or the size of the dislocation cells observed in the specimen at 0.7 fatigue life. This result is consistent with the theory of extrusions and intrusions formation during fatigue crack propagation [9].

REFERENCES

[1]   Nageshaa A., Valsana A. M., Kannana R., Bhanu Sankara Raoa K., Bauerb V., Christc H.-J., Singhd V. Thermomechanical Fatigue Evaluation and Life Prediction of 316L(N) Stainless Steel. International Journal of Fatigue, Vol. 31, 2009, p. 636-643.

[2]   Ramesh M.,Hans J. L., Diener M., Spolenak R. Conducting Thermomechanical Fatigue Test in Air at Light Water Reactor Relevant Temperature Intervals. Journal of Nuclear Materials, Vol. 415, 2011, pp. 23-30.

[3]   Fekete B., Kasl J., jandova D., Jóni B., Misják F., Trampus P. Low Cycle Thermomechanical Fatigue of Reactor Steels: Microstructural and Fractographic Investigations. Material Science and Engineering A (in print).

[4]   Keh A. S., Weismann S. Electron Microscopy and Strength of Crystals. New York: Wiley, 1963, p. 231.

[5]   Nakata K., Okada O., Ueki Y., Kamino T. Effects of Foil Thickness on Measurement of Grain Boundary Segregation with FEG-TEM/EDS in Austenitic Stainless Steels. Journal of Electron Microscopy, Vol. 47 (3), 1998, pp. 193 - 200.

[6]   Hirsch P.B., Howie A., Nicholson R.B., Pashley D.W., Whelan M.J. Electron Microscopy of Thin Crystals, Butterworths: London, 1965, p.423

[7]   Kettunen P.O., Kuokkala V.-T. Plastic deformation and strain hardening. Materials Science Foundations, Vol. 16-18, Trans Tech Publications Ltd., 2003. pp. 304-393

[8]   Mughrabi H., Ackermann F., Herz K. Persistent Slip Bands in Fatigued Face-Centered and Body-Centered Cubic Crystals. In Fatigue mechanism, J.T. Fong Eds., ASTM-STP 675, American Society for Testing Materials, 1979. pp. 69-105.

[9]   BROWN L.M. Crack and Extrusions Caused by Persistent Slip Bands. Philosophical Magazine, Vol. 92, Nos. 28-30, 2013, pp.3809-3820.